"Physics of Auroral Phenomena", Proc. XLIV Annual Seminar, Apatity, pp. 12-15, 2021

Polar Geophysical Institute

DOI: 10.51981/2588-0039.2021.44.002

SUPERSUBSTORM ON 28 MAY 2011 – GEOMAGNETIC EFFECTS IN THE GLOBAL SCALE

I.V. Despirak[1], N.G. Kleimenova[2], A.A. Lubchich[1], P.V. Setsko[1], R. Werner[3]

[1]*Polar Geophysical Institute, Apatity, Russia;* e-mail: *despirak@gmail.com*
[2]*Schmidt Institute of the Physics of the Earth, RAS, Moscow, Russia*
[3]*Space Research and Technology Institute, Bulgarian Academy of Sciences, Bulgaria*

Abstract. For this analysis, we selected the supersubstorm (SSS) occurred during the strong magnetic storm on 28 May 2011 (SYM/H~100 nT). The ground-based magnetic effects of SSS have been studied basing on the data from the global SuperMAG, INTERMAGNET and IMAGE magnetometer networks, as well as on the magnetic measurements by the ionospheric satellite AMPERE system. According to the SML- index behavior, the SSS event maximum was identified at ~09:00 UT on 28 May 2011 (SML= ~-2600 nT). The SSS occurred during the passage of the magnetic cloud in the solar wind. Before the SSS, the B_Z component of the Interplanetary Magnetic Field (IMF) was negative, the IMF B_Y component was positive, and the local jump in the solar wind dynamic pressure was registered. We found that the SSS developed in the magnetosphere in the global scale. A strong westward electrojet was observed at auroral latitudes from the evening side to the dayside. In contrast to the typical scenario of a classical substorm, a very intense eastward electrojet was detected in the afternoon-evening sector. That may be a result of the formation of an additional partial ring current during the supersubstorm.

Introduction

For the first time the term "supersubstorm" was introduced in the study of very intense magnetic substorms from the data of the SuperMag magnetometers network, the events with high negative values of the SML index (< - 2500 nT) were called "supersubstorms" [1]. The SML index is calculated across the network of the SuperMAG stations globally located from 40° to 80° MLat, and therefore contains not only the standard stations of the auroral zone but also many other stations [2]. First studies of supersubstorms were devoted to the investigations of conditions of their appearance. So, the seasonal variations and dependence on the solar activity were considered and was shown that the SSS events can be observed during any phase of the solar cycle, but their highest frequency of the occurrence observed in the declining phase of the solar activity cycle [3]. The following investigations showed that the SSS events are not always associated with very intense storms and can be observed also during less intense (-100 nT $\geq$ Dst > -250 nT) and moderate magnetic storms (-50 nT $\geq$ Dst > -100 nT), and even during non-storm (Dst > -50 nT) intervals [3], [4]. It was shown also that the supersubstorms are observed during the definite solar wind types - magnetic clouds (MC) and SHEATH plasma compression regions ahead of MCs - and practically not observed during another streams and structures of the solar wind [4]. The initial studies of auroral disturbances showed that the development of auroras differs significantly from the classical pattern of substorm development. It is not seen the standard brightening of the equatorial arc in the midnight sector and breakup of auroras. However, there were intense auroras in the pre-midnight and morning sectors of the magnetic local time (MLT) [5]. Note that it will be confirmed later by the analysis of the SSS development on 5 April 2010 [6]. The electojets development during the supersubstorms has been considered in some works [7], [8], [9]. It was shown that the westward electrojet during two supersubstorms on 8 September 2017 developed on a global scale by the longitude from the prenoon to the afternoon sector surrounding the Earth. The highest intensity of the electrojet was observed at the auroral latitudes in the post-midnight time [7]. Similar spatial features of electojets were presented in [8] and [9], where we analyzed two supersubstorms during the magnetic storm of March 9, 2012 and one supersubstorm during the magnetic storm of 5 April 2010. It is shown also that the strong eastward current observed from after-noon to evening sector, the occurrence of the intense eastward electrojet supports the hypothesis of the formation of the additional ring current in the evening sector during SSS [10].

Here we analyzed the appearance of one more SSS event observed during the magnetic storms on 28 May 2011. It is one of the few isolated SSS event, which have been observed since 2010. The purpose of this work is to investigate the features of the global spatial distribution of electrojets during this supersubstorm and to verify the assumption about the development of a strong partial ring current during SSS.

Data

For this purpose, the ground-based magnetic data from the SuperMAG, INTERMAGNET and IMAGE networks were combined with the magnetic registrations data of AMPERE satellites and CDAWeb database. The solar wind

and IMF parameters were taken from the CDAWeb database and catalog of large-scale solar wind types ftp://ftp.iki.rssi.ru/pub/omni/catalog. The IMAGE magnetometer data were taken from http://space.fmi.fi/image/. Supersubstorm onset and its development were determined by using the geomagnetic indexes SML, SMR and SMR_LT from http://supermag.jhuapl.edu/. The SMR index calculation (as SymH index) is based on the data of the N component with the baseline removed at available (~100 stations) ground magnetometer stations at geomagnetic latitudes between -50 and +50 degrees. Four local time sectors are defined with centers at 00, 06, 12, 18 MLT; the SMR value is (SMR-00 + SMR-06 + SMR-12 + SMR-18)/4/ [11]. The global spatial distribution of electrojets was determined from the maps of magnetic field vectors obtained on the SuperMAG network, maps of spherical harmonic analysis of the distribution of magnetic vectors in the ionosphere and field-aligned currents obtained from the data of the 66 low-apogee communication satellites Iridium of the AMPERE system (Active Magnetosphere and Planetary Electrodynamics Response Experiment http://ampere.jhuapl.edu).

Results

1. Interplanetary and geomagnetic conditions

Solar wind and interplanetary magnetic field (IMF) conditions for period 02-17 UT on 28 May 2011 are shown in the Fig. 1a, from the top to bottom: IMF magnitude (B_T), the IMF Y- and Z- components (B_Y, B_Z), the flow velocity (V), the dynamic pressure (P) and some geomagnetic indexes as the PC, SYM_N/H and SML. It is seen that the features of a coronal mass ejection (CME) are observed in this time period – the SHEATH and magnetic cloud (MC), whose boundaries are marked by the horizontal arrows. The MC contains a long-lasting interval of negative values of the IMF B_Z, which could have caused the development of a strong magnetic storm (Dst~100 nT). Against the background of this magnetic storm, at ~08 UT one supersubstorm (SSS) began to develop. The moment of the SSS onset is shown by the vertical redhead line. It can be seen that the SSS was developed at the main phase of the storm, during the magnetic cloud (MC). Ahead of the SSS, a local pressure jump was observed; the IMF B_Z was negative, the IMF B_Y was positive, the PC- index has grown very strongly, which indicated a very large supply of energy from the solar wind.

To describe the global development of the magnetic supersubstorm, we applied the geomagnetic ring current index (SMR), separated by the MLT sectors (SMR_LT), which is shown in Fig. 1b. The SML and MPB indices are shown for comparison. Besides, the MPB index representing the power of midlatitude positive magnetic bays was calculated only for the midlatitude station Panagyurishte (PAG). It is seen that during the supersubstorm, there was a strong enhancement of the ring current in the evening sector (violet curve), i.e., the strong current asymmetry appeared. We suppose that it was due to the additional partial ring current development. It can also be seen that a strong increase in the horizontal power was observed at Panagyurishte station; the power value was comparable in magnitude to those observed during substorms [12].

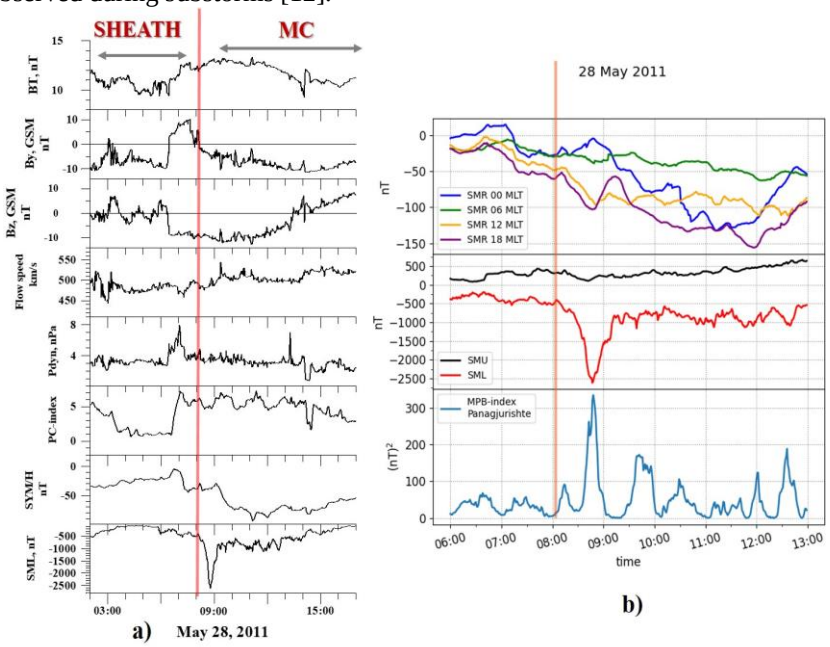

Figure 1. Variations of the solar wind and IMF parameters (B_T, B_Y, B_Z, V, P_{dyn}) and some geomagnetic indexes (PC, SYM/H, SML) from 02 to 17 UT on 28 May 2011 (a) and additional geomagnetic indexes (SMR_LT, SMU, SML) and horizontal power of midlatitude positive bays (MPB) on the Panagyurishte station from 06 to 13 UT on 28 May 2011 (b). The boundaries of the solar wind types are marked by the horizontal arrows and inscriptions: SHEATH and MC. The moment of the SSS onset is shown by the vertical redhead line.

2. Geomagnetic observations

Ground-based magnetic disturbances during SSS are shown in Fig. 2. At the top panel, the global maps of magnetic field vectors by SuperMag data there are shown for 3-time moments, from the onset to the maximal SSS development (Fig.2a). It is seen that strong disturbances were observed over Alaska, very intense negative magnetic bays started at ~ 08:30 UT; the intensity of the negative bays was ~ -1300-2500 nT (Fig.2b). The positive magnetic bays with the intensity of ~ 70-250 nT were registered at East Siberian and Kamchatka stations (YAK, MGD, PET). So, the westward electrojet during the SSS developed in the global scale (from before midnight, through the night and morning, and into the day sector). Besides, the strong eastward electrojet was observed in the evening sector.

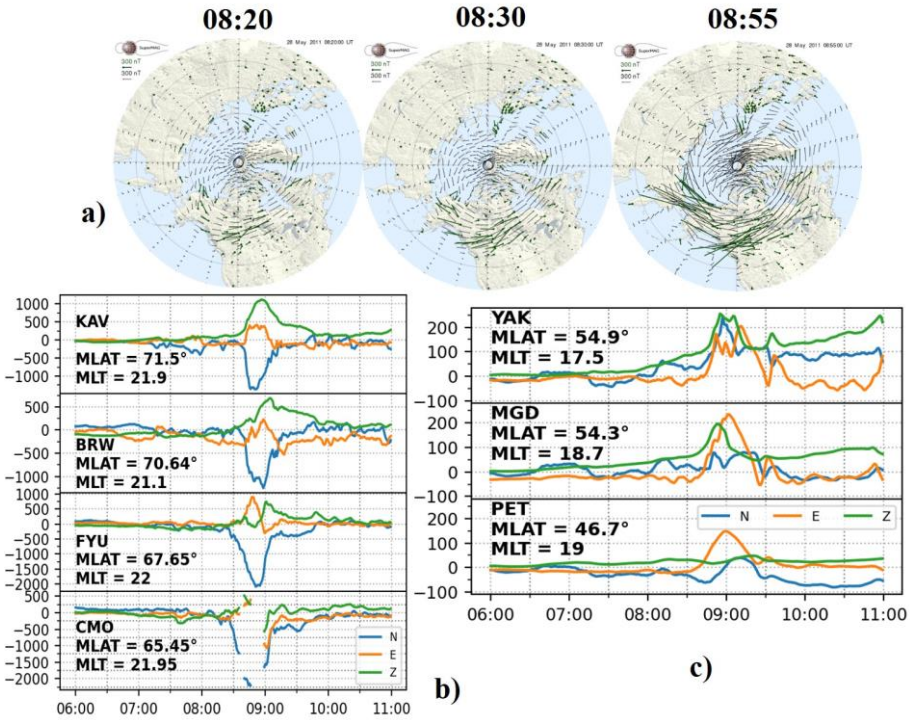

Figure 2. Global maps of the spatial distribution of magnetic field vectors from the SuperMAG network at 08:20, 08:30 and 08:55 UT (a); magnetograms of some stations on Alaska (b) and on Siberian (c) from 06 to 11 UT on 28 May 2011.

3. Field-aligned currents from AMPERE observations and models of SCW

Two panels of the AMPERE maps on 28 May 2011 for different time (at ~ 08:30 UT and ~ 08:55 UT) are shown in Figure 3a. The AMPERE project represents the results of the magnetic registrations by the 66 satellites at 700 km altitude, its spherical harmonic analysis (the middle map) and calculated Field Aligned Currents (FAC) distribution. The upward currents mark by red, the downward ones – by blue. Note, that the westward current was located between the upward (red) and downward (blue) FAC; the eastward electojet was located between downward (blue) and upward (red) currents. It is seen the global longitude expansion of the westward electrojet - from the evening side at auroral latitudes to the day side of the polar area. The AMPERE maps demonstrate also very strong enhancement of the eastward electrojet in the afternoon-evening sector and its shift to the lower latitudes.

It should be noted that the occurrence of the strong eastward electrojet in the evening sector supports the hypothesis of the formation of the additional ring current in the evening sector during SSS [11]. *Zong et al.* [2021] proposed, that substorm current wedge (SCW) for supersubstorms differs significantly from the classical pattern of SCW development. Two SCW models are presented in Figure 3b (taken from [11]), left panel shows the SCW model for "classical" substorm, the right panel - for a supersubstorm. It is seen, that during SSS on 28 May 2011, the very intense eastward electrojet in the evening sector was detected. In contrast to the typical scenario of the classical substorm, it may be the result of the formation of an additional partial ring current during the supersubstorm.

Conclusions

1) We found that during the SSS of May 28, 2011, a strong westward electrojet was observed in the evening and night sectors globally - from the evening side at auroral latitudes to the dayside of the Earth.

2) During this SSS, an intense eastward electrojet in the evening sector was detected as well. We support that it could be a result of the formation of an additional partial ring current occurred during a supersubstorm.

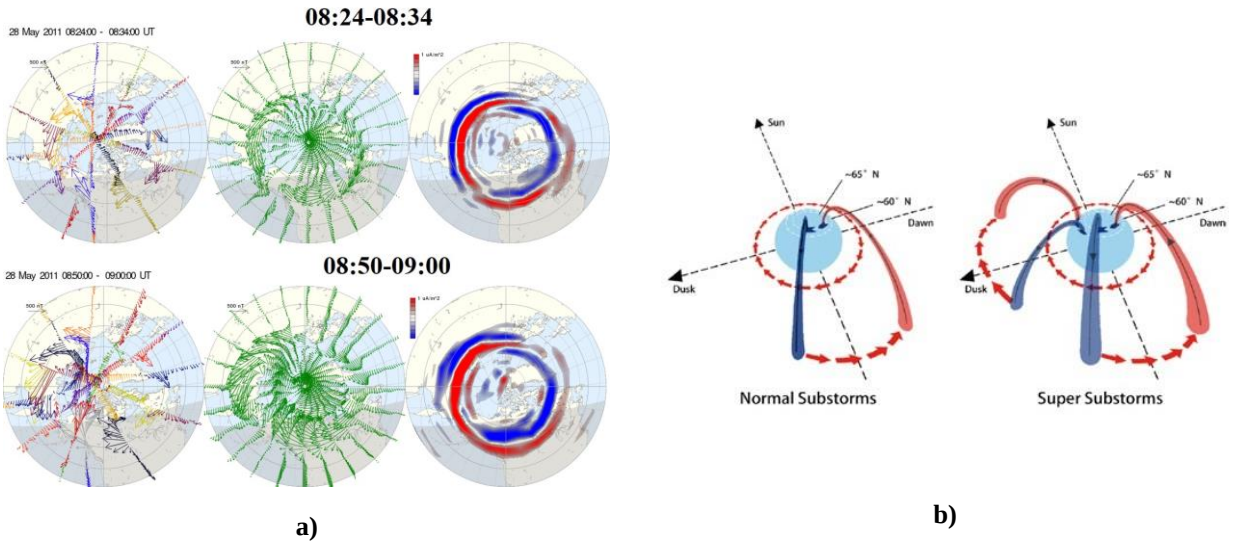

Figure 3. Distribution of magnetic disturbance vectors, their spherical harmonic analysis and field-aligned current distribution for two moments (at ~ 08:30 UT and ~ 08:55 UT) on May 28, 2011 according to AMPERE data (a); models of substorm current wedge (SCW) for normal substorm and for supersubstorm (b).

Acknowledgements

The authors are grateful to the creators of the OMNI databases (http://omniweb.gsfc.nasa.gov), SuperMAG (http://supermag.jhuapl.edu/) and AMPERE (http://ampere.jhuapl.edu) for the ability to use them in our work. The work of I.V. Despirak, N.G. Kleimenova, A.A. Lubchich, P.V. Setsko. was carried out within the framework of the RFBR grant No. 20-55-18003_Bulg_a; R. Werner's work was carried out within the framework of the project of the National Science Foundation of Bulgaria (project No. KP-06Rusia / 15).

References

1. Tsurutani B.T., Hajra R., Echer E., Gjerloev J.W. (2015). Extremely intense (SML≤ −2500 nT) substorms: isolated events that are externally triggered? *Ann. Geophys.*, 33, 519–524.
2. Gjerloev J.W. (2012). The SuperMAG data processing technique. *J. Geophys. Res.*, 117(A9), A09213. https://doi.org/10.1029/2012JA017683
3. Hajra R., Tsurutani B.T., Echer E., Gonzalez W.D., Gjerloev J.W. (2016). Supersubstorms (SML <-2500 nT): Magnetic storm and solar cycle dependences. *J. Geophys. Res. Space Physics*., 121, 7805–7816. doi:10.1002/2015JA021835
4. Despirak I.V., Lyubchich A.A., Kleimenova N.G. (2019). Supersubstorms and conditions in the solar wind. *Geomag. Aeron*., 59, no. 2, 170-176.
5. Hajra R., Tsurutani B.T. (2018). Interplanetary shocks inducing magnetospheric supersubstorms (SML < –2500 nT): Unusual auroral morphologies and energy flow. *Astrophys. J*., 858, no. 2, id 123. https://doi.org/10.3847/1538-4357/aabaed
6. Nishimura Y., Lyons L.R., Gabrielse C., Sivadas N., Donovan E.F., Varney R.H., Angelopoulos V., Weygand J.M., Conde M.G., Zhang S.R. (2020). Extreme magnetosphere-ionosphere-thermosphere responses to the 5 April 2010 supersubstorm. *J. Geophys. Res*., 125, no. 4. https://doi.org/10.1029/2019JA027654
7. Despirak I.V., Kleimenova N.G., Gromova L.I., Gromov S.V., Malysheva L.M. (2020). Supersubstorms during storms of September 7–8, 2017. *Geomag. Aeron.*, 60, no. 3, 308-317.
8. Despirak I.V., Lubchich A.A., Kleimenova N.G., Gromova L.I., Gromov S.V., Malysheva L.M. (2021). Longitude geomagnetic effects of the supersubstorms during the magnetic storm of March 9, 2012. *Bulletin of the Russian Academy of Sciences: Physics*., 85, no. 3, 246–251.
9. Despirak I.V., Kleimenova N.G., Gromova L.I., Lubchich A.A., Guineva V., Setsko P.V. Spatial features of supersubstorm in the main phase of the magnetic storm on 5 April 2010. *Bulletin of the Russian Academy of Sciences: Physics*, 2022 (in press)
10. Zong Q.-G., Yue C., Fu S.-Y. (2021). Shock induced strong substorms and super substorms: Preconditions and associated oxygen ion dynamics. *Space Science Review*, 217. https://doi.org/10.1007/s11214-021-00806-x
11. Newell P.T., Gjerloev J.W. (2011). Evaluation of SuperMAG auroral electrojet indices as indicators of substorms and auroral power. *J. Geophys. Res.: Space Phys.*, 116, no. A12, A12211.
12. Werner R., Guineva V., Atanassov A., Bojilova R., Raykova L., Valev D., Lubchich A., Despirak I. Calculation of the horizontal power perturbations of the Earth surface magnetic field. *Proceedings of the Thirteenth Workshop "Solar Influences on the Magnetosphere, Ionosphere and Atmosphere"*, Primorsko, Bulgaria, 13-17 September, 2021 (in press).